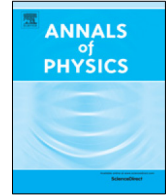




Contents lists available at ScienceDirect

## Annals of Physics

journal homepage: [www.elsevier.com/locate/aop](http://www.elsevier.com/locate/aop)

# Strange metal state near quantum superconductor-metal transition in thin films<sup>☆</sup>

Konstantin S. Tikhonov, Mikhail V. Feigel'man<sup>\*</sup>

L. D. Landau Institute for Theoretical Physics, Chernogolovka, 142432, Moscow region, Russia  
Skolkovo Institute of Science and Technology, Moscow 143026, Russia

## ARTICLE INFO

## Article history:

Received 19 February 2020

Received in revised form 26 February 2020

Accepted 6 March 2020

Available online 31 March 2020

## ABSTRACT

We develop a theory of quantum  $T = 0$  phase transition (q-SMT) between metal and superconducting ground states in a two-dimensional metal with frozen-in spatial fluctuations  $\delta\lambda(r)$  of the Cooper attraction constant. When strength of fluctuations  $\delta\lambda(r)$  exceeds some critical magnitude, usual mean-field-like scenario of the q-SMT breaks down due to spontaneous formation of local droplets of superconducting phase. The density of these droplets grows exponentially with the increase of average attraction constant  $\lambda$ . Interaction between the droplet's order parameters is due to proximity effect via normal metal and scales with distance  $\propto 1/r^\beta$ , with  $2 < \beta \leq 3$ . We account for this interaction by means of a real-space strong-disorder renormalization group (RG). Near the q-SMT the RG flow is, formally, a dual equivalent of the Kosterlitz-Thouless RG. The corresponding line of fixed points describes a Griffiths phase of a metal with large fractal clusters of superconducting islands. Typical number of islands in a cluster grows as  $N_\delta \sim 1/\delta$ , where  $0 < \delta \ll 1$  is the distance to the critical point. Superconducting side is described by a runaway of RG trajectories into the strong-coupling region. Close to the transition point on the SC side,  $0 < -\delta \ll 1$ , RG trajectories possess an extremum as function of the RG parameter  $|\delta|^{1/2} \ln(1/T\tau)$ . It results in a wide temperature range where physical properties are nearly  $T$ -independent. This observation may be relevant to the understanding of a *strange metal* state frequently observed near q-SMT.

© 2020 Elsevier Inc. All rights reserved.

<sup>☆</sup> This article is part of the Special Issue: Eliashberg theory at 60.

<sup>\*</sup> Corresponding author at: L. D. Landau Institute for Theoretical Physics, Chernogolovka, 142432, Moscow region, Russia.

E-mail address: [feigel@landau.ac.ru](mailto:feigel@landau.ac.ru) (M.V. Feigel'man).

## 1. Introduction

A number of potentially superconducting materials and alloys lose their superconducting properties upon increase of disorder-induced electron scattering, suppressing superconducting transition temperature  $T_c$  to zero. The resulting state may be either insulating, with a metallic state right at the quantum critical point, or metal-like in the whole range of parameters. The first situation is referred to as Superconductor–Insulator Transition (SIT) [1,2], while the second one as Superconductor–Metal Transition (SMT). In this paper we will study SMT in two-dimensional (2D) or quasi-2D disordered materials.

It is usually assumed that a genuine metallic state cannot exist in 2D due to Anderson localization. However, the corresponding localization length is exponentially long for not too strong disorder:  $L_{\text{loc}}^{2D} \sim l e^{\pi g/2}$  where  $g = h/e^2 R_{\square}$  is the dimensionless conductance of the film at high temperatures (when semiclassical Drude law is applicable) and  $l$  is the elastic mean free path for electrons. The corresponding energy (and temperature) scale where localization becomes relevant equals  $T_{\text{loc}} \sim \tau^{-1} \exp(-\pi g)$ , where  $\tau$  stays for elastic scattering time. Below we consider situations when  $g \gg 1$  is sufficiently large and thus exponentially low  $T_{\text{loc}}$  can be treated as zero, since all temperatures in our problem will be much higher. Under such an assumption, it is legitimate to consider  $T = 0$  metal state and quantum phase transition of the SMT type in 2D (which may become SIT transition if the temperature is reduced below  $T_{\text{loc}}$  [3]).

A natural mechanism of SMT transition upon increase of potential disorder is due to increase of effective Coulomb repulsion between slowly diffusing electrons [4,5]. The corresponding critical value  $g_c$  of the Drude conductance  $g$  equals  $g_c = \frac{1}{2\pi} \ln^2 \frac{1}{T_{c0}\tau}$  (with  $T_{c0}$  for the superconducting transition temperature of the same material in the clean limit), and can be rather large,  $g_c \approx 10$ . This mechanism is known to describe quite well the major features of the SMT in a number of materials with high electron density and high disorder, like amorphous  $\text{Mo}_x\text{Ge}_{1-x}$ ,  $\text{Nb}_x\text{Si}_{1-x}$  and many other. An extension of the Finkel'stein theory [4,5] was developed to treat inhomogeneous systems composed of small superconducting islands in contact with dirty metal [6–8]. Such an approach allows to locate the SMT position depending on the system parameters (conductance  $g$ , fraction of superconducting regions  $x \ll 1$ , etc.)

However, the nature of the ensuing metal phase realized at  $g < g_c$  at very low temperatures is not understood yet. Strong enhancement of conductance (compared to its magnitude in the normal state  $g$ ) is frequently observed [9] in the vicinity of a quantum transition to superconducting state. Surprisingly, conductance is weakly  $T$ -dependent in this phase dubbed therefore ‘strange metal’. In some cases [10], strange metal state has been shown to have extrinsic origin (insufficient filtering of high-frequency noise in the measuring system). However, it is not clear if all numerous observations of a ‘strange metal’ state are of the same origin. In the present paper we discuss another possible origin of the strange metal behavior: a  $T = 0$  Griffiths phase dominated by large statistical fluctuations due to frozen-in fluctuations of the Cooper interaction amplitude.

To derive these new results, we employ a model of a diffusive metal with relatively large conductance  $g$  and spatially fluctuating Cooper interaction  $\lambda(\mathbf{r}) = \bar{\lambda} + \delta\lambda(\mathbf{r})$  ( $\lambda > 0$  corresponds to attraction). We find that at sufficiently strong fluctuations  $\delta\lambda(\mathbf{r})$  characterized by “disorder strength”  $w$  (to be defined precisely below) an unusual type of quantum SMT occurs upon increase of the mean value of the Cooper interaction  $\bar{\lambda}$ .

The rest of the paper is organized as follows. In Section 2 we formulate and study a special kind of Anderson localization problem that describes eigenvalue spectrum and eigenfunctions of the propagator of superconducting fluctuations  $L(\mathbf{r}, \mathbf{r}')$  within the random- $\lambda$  model. We present numerical results for the spectrum density  $\rho(E)$  and statistical properties of the eigenfunctions  $\psi_E(\mathbf{r})$  related to the  $L(\mathbf{r}, \mathbf{r}')$ . It will be shown that eigenfunctions near the lower edge of the spectrum  $E_0$  (defined as  $\rho(E) = 0$  at  $E < E_0$ ) are extended at relatively small strength of disorder,  $w$ , but localized at large enough  $w$ ; these qualitatively different regimes are separated by the critical disorder strength  $w_c$ .

Thus the nature of q-SMT is determined by *emergent superconducting granularity*. Note the difference between this phenomenon and previously studied superconducting granularity that is

due to strong random potential scattering of electrons [11–15] and occurs near SIT. In the model we discuss in the present paper superconducting islands occur within a ‘sea’ of a normal metal.

In Section 3 we extend our analysis to non-linear and non-local terms of the dynamic Ginzburg–Landau action. We study phase dynamics of individual superconducting islands and derive an effective interaction between phases of *different* localized islands. We show that this interaction is of the same functional form that is known for proximity-induced Josephson coupling between artificially prepared superconducting islands on top of diffusive 2D metal, analyzed previously in Refs. [6–8,16]. Upon increase of mean Cooper attraction  $\bar{\lambda}$ , this interaction becomes strong enough to produce correlations between phases of different islands. At this stage, a macroscopic description of superconducting correlations on a length scale containing many original islands becomes necessary.

To treat these correlations quantitatively, in Section 4 we use a version of Strong-Disorder Renormalization Group (SDRG), originally due to D. S. Fisher [17,18], and extensively reviewed in [19–21]. We find our problem to be formally similar to the one studied in Ref. [22] and identify disordered Griffiths phase with a line of fixed points of the SDRG transformations. Long-range interaction between localized islands of superconductivity leads to formation of strongly coupled fractal clusters of islands with a slow collective dynamics. Superconducting phase is then identified with a runaway of the SDRG solution into the strong-coupling regime and generation of a long-but-finite spacial scale where macroscopic superconducting coherence sets in. In Section 5 we discuss low-temperature physics of the strange metal and superconducting phases. Finally, Section 6 is devoted to the discussion of results and conclusions. Supplemental material Sections (S1 and S2) contain a number of technical details of our theory.

## 2. Anderson localization of superconducting modes

### 2.1. Model

We consider a model of normal metal with moderately large dimensionless conductance  $g \gg 1$ , with phonon-mediated Cooper attraction characterized by BCS coupling strength  $\lambda_*$ . Coulomb interaction between electrons is considered to be in the ‘universal limit’, i.e. screened static Coulomb potential is equal to  $v^{-1}$ , where  $v$  is the electron density of states (per single spin projection). The effect of Coulomb interaction and disorder upon superconducting instability threshold [4,5] can be represented [7,23] via effective repulsion constant  $\lambda_g = 1/\sqrt{2\pi g} \ll 1$ . It is important to notice that effective repulsion  $\lambda_g$  cannot be simply subtracted from the attraction constant  $\lambda_*$ . Indeed, superconducting instability due to the presence of  $\lambda_*$  can be described by summation of ladder diagrams within Cooper channel only (electron processes with a small total momentum of electron pair). On the other hand, Coulomb interaction enters via the density-density channel, and it is necessary to take into account non-ladder diagrams of ‘parquet’ type. In the mean-field scenario, quantum phase transition from metal to superconducting state occurs upon increase of the average attraction  $\langle \lambda_* \rangle$  against the background of repulsion whose strength is determined by  $\lambda_g$ .

The stability of the normal state with respect to the effect of superconducting inclusions is determined by the properties of superconducting propagator  $L(\omega, q)$ . The quadratic part of the Ginzburg–Landau (GL) functional reads

$$S_2 = \int \frac{d\omega}{2\pi} \int d\mathbf{r}_1 d\mathbf{r}_2 \Delta_\omega(\mathbf{r}_1) \Pi(\omega, \mathbf{r}_1 - \mathbf{r}_2) \Delta_\omega(\mathbf{r}_2). \quad (1)$$

We start with expression for  $\Pi(\omega, \mathbf{q})$  at  $\omega = 0$  and in homogeneous system. Technically it is convenient to account for the effect of Coulomb repulsion on the Cooper channel in the way it was done in Refs. [24,25]. Namely, we introduce the Cooperon screening factor  $w_q(\epsilon)$  which modifies usual expression for the Cooperon amplitude  $C_q(\epsilon) = v/(Dq^2 + 2|\epsilon|)$  multiplicatively:  $C_q(\epsilon) \rightarrow C_q(\epsilon)w_q(\epsilon)$ . In the limit of  $T \rightarrow 0$ , the screening factor  $w_q(\epsilon)$  obeys then the following equation:

$$w_q(\epsilon) = 1 - \int \frac{d\epsilon_1}{2\pi} \frac{2\theta(\epsilon\epsilon_1)}{g} \ln \frac{1}{|\epsilon + \epsilon_1|\tau} \frac{w_q(\epsilon_1)}{Dq^2 + |\epsilon_1|}, \quad (2)$$

where  $\theta(x)$  is the Heaviside step function. Eq. (2) for the function  $w_q(\epsilon) \equiv w_q(\zeta)$ , with  $\zeta = \ln(1/\epsilon\tau)$ , can be rewritten (within the logarithmic accuracy) in the following form:

$$w_q(\epsilon) = 1 - \lambda_g^2 \int_0^{\zeta_q} d\zeta_1 \min(\zeta, \zeta_1) w_q(\zeta_1), \quad (3)$$

where  $\zeta_q = -2 \ln(ql)$ . Solution of Eq. (3) with initial condition  $w_q(0) = 1$  is

$$\begin{aligned} w_q(\zeta \leq \zeta_q) &= \cosh(\lambda_g \zeta) - \tanh(\lambda_g \zeta_q) \sinh(\lambda_g \zeta), \\ w_q(\zeta \geq \zeta_q) &= \frac{1}{\cosh(\lambda_g \zeta_q)}. \end{aligned} \quad (4)$$

The Cooperon screening factor modifies  $\Pi(0, \mathbf{q})$  as follows:

$$\Pi(0, \mathbf{q}) = \frac{\nu}{\lambda_*} - \int d\epsilon \frac{\nu}{Dq^2 + 2|\epsilon|} w_q(\epsilon). \quad (5)$$

Substitution of Eq. (4) into Eq. (5) and integration leads to (we also account for finite frequency  $\omega$ )

$$\Pi(\omega, \mathbf{q}) = \frac{\nu}{\lambda_*} - \frac{\nu}{\lambda_g} + \frac{\nu}{\lambda_g} \Pi_0(\omega, \mathbf{q}), \quad (6)$$

with

$$\Pi_0(\omega, \mathbf{q}) = \frac{2}{1 + [(ql)^2 + 2\omega\tau]^{-2\lambda_g}}, \quad (7)$$

which at  $ql \ll 1$ ,  $\omega\tau \ll 1$  becomes  $\Pi_0(\omega, \mathbf{q}) \approx 2 [(ql)^2 + 2\omega\tau]^{2\lambda_g}$ . Now we account for spatial fluctuations of the bare Cooper attraction constant  $\lambda_*$  and replace the function  $\Pi(\omega, \mathbf{q})$  by the operator

$$\hat{\Pi}(\omega, \mathbf{q}; \mathbf{r}) = \frac{\nu}{\lambda_g} \left[ \frac{\lambda_g}{\lambda_*(\mathbf{r})} - 1 + \Pi_0(\omega, \mathbf{q}) \right] \quad (8)$$

It is more convenient to parametrize the disorder as

$$\frac{\lambda_g}{\lambda_*(\mathbf{r})} - 1 = \delta_0 + u(\mathbf{r}), \quad (9)$$

assuming that random field  $u(\mathbf{r})$  has zero mean and

$$\delta_0 = \left\langle \frac{\lambda_g}{\lambda_*(r)} \right\rangle - 1 \quad (10)$$

is the bare distance to superconductor-metal transition at  $T = 0$ . We will assume  $u(\mathbf{r})$  to be Gaussian with correlation function  $\overline{u(\mathbf{r})u(\mathbf{r}')} = \Lambda f(|\mathbf{r}|/b)$  (although by definition  $u(\mathbf{r}) \geq -1 - \delta_0$ , this constraint is not problematic, as we discuss below). Here  $\Lambda$  is the dimensionless fluctuation strength and  $b$  is the correlation length, while function  $f(x)$  is assumed to be fast decaying at  $x \geq 1$  and normalized according to  $\int f(x) d^2x = 1$ . It turns out the properties of  $L(r)$  depend crucially on the value of dimensionless parameter  $w = \Lambda b^2/l^2$ , which is determined by both the fluctuations of  $\lambda_*(\mathbf{r})$  and the electronic mean free path  $l$ . Disorder correlation length  $b$  can be larger than  $l$ , but  $b$  is always smaller than localization length of eigenstates discussed below.

The superconducting propagator  $L(\omega, \mathbf{q})$  is given by the Fourier transform of the average solution  $\mathcal{L}(\omega; \mathbf{r}, \mathbf{r}')$  of the equation

$$\begin{aligned} (\delta_0 + u(\mathbf{r})) \mathcal{L}(\omega; \mathbf{r}, \mathbf{r}') + \int d^2\mathbf{r}_1 \Pi_0(\omega, \mathbf{r} - \mathbf{r}_1) \mathcal{L}(\omega; \mathbf{r}_1, \mathbf{r}') \\ = \frac{\lambda_g}{\nu} \delta(\mathbf{r} - \mathbf{r}'). \end{aligned} \quad (11)$$

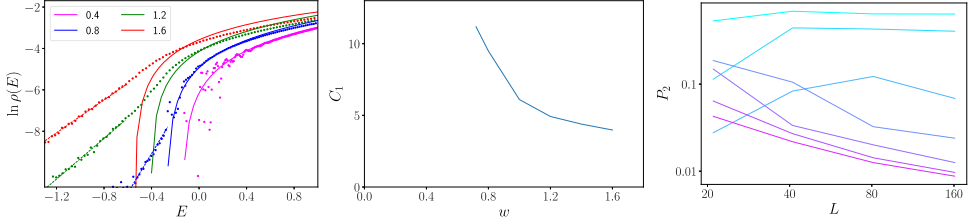


**Fig. 1.** Characterization of the eigenstates of Eq. (13) at  $\lambda_g = 0.2$  and several values of disorder  $w$ . a: DoS  $\rho(E)$  found from ED (dots), disorder  $w$  is indicated on the legend. Solid lines:  $\rho(E)$  as found from SCBA, Eqs. (14) and (15). In the tail: dashed lines are fits by Eq. (18). b:  $w$ -dependence of the coefficient  $C_1$  in Eq. (18); we expect  $w_c$  to be in the interval (0.4 – 0.5). c: Inverse participation ratio  $P_2$  at  $w = 1.2$  for several energies  $E = -0.8, -0.6, -0.4, -0.2, 0.0, 0.2, 0.4$  from cyan to magenta. Observe that states become less localized upon increasing the energy  $E$  from the tail to the bulk of the spectrum. (For interpretation of the references to color in this figure legend, the reader is referred to the web version of this article.)

As a result,

$$L_\omega(\mathbf{r} - \mathbf{r}') = \overline{\mathcal{L}(\omega, \mathbf{r}, \mathbf{r}')} = \frac{\lambda_g}{v} \overline{\sum_n \frac{\psi_n(\mathbf{r})\psi_n^*(\mathbf{r}')}{E_n + \delta_0 - i0}}, \tag{12}$$

where  $\psi_n(\mathbf{r})$  and  $E_n$  are determined by the following equation:

$$\int d^2\mathbf{r}_1 [\Pi_0(\omega, \mathbf{r} - \mathbf{r}_1) + u(\mathbf{r})\delta(\mathbf{r} - \mathbf{r}_1)]\psi_n(\mathbf{r}_1; \omega) = E_n\psi_n(\mathbf{r}; \omega). \tag{13}$$

To avoid confusion, we emphasize that variable  $E$  in the above equation (and below) has nothing to do with single-electron energies.

The critical point of the mean-field transition is determined by the divergence of  $L(\omega \rightarrow 0, q \rightarrow 0)$ . In the absence of Cooper constant fluctuations,  $w = 0$ , it occurs at  $\delta_0 = 0$ . Relatively weak fluctuations  $u(\mathbf{r})$  shift it to some nonzero  $\delta_c$ , as long as eigenfunctions  $\psi_n(\mathbf{r})$  remain delocalized near the band edge, i.e. for smallest values of eigenvalues  $E_n$  of the operator (13) at  $\omega = 0$ . In this case  $\delta_c = -\min(E_n)$ . Below we find, at sufficient increase of  $w$ , localization of eigenfunctions with eigenvalues close to the spectral edge, invalidating this simplest mean-field scenario.

### 2.2. Numerical analysis

We start from evaluation of the Density of States (DoS) of the operator defined by Eq. (13), in the self-consistent Born approximation (SCBA). DoS  $\rho(E)$  is then determined by the following equation:

$$\rho(E) = \frac{1}{4\pi^2} \text{Im} \Sigma(E + \sigma(E)), \tag{14}$$

where  $\sigma(E)$  can be found from nonlinear self-consistency equations

$$\begin{aligned} \sigma(E) &= w^2 \Sigma(E + \sigma(E)), \\ \Sigma(E) &= \frac{1}{2\pi} \int_0^1 \frac{(ql)d(ql)}{-E + \Pi_0(0, q)}. \end{aligned} \tag{15}$$

Notice that disorder enters Eq. (15) via the parameter  $w = \Lambda b^2/l^2$ , where factor  $1/l^2$  appears due to the high-momentum cutoff  $q_{\text{max}} = 1/l$  in the integral. Solving Eq. (15) numerically and evaluating the DoS in Eq. (14), we find the results, presented in Fig. 1a by solid lines for several values of disorder. According to these results, the sharp edge of the eigenvalue spectrum survives within SCBA approximation, and the position of this edge is  $-\delta_c(w)$ . For  $\lambda_g = 0.2$ , the function  $\delta_c(w)$  was determined numerically to be  $\delta_c(w) = 0.34w$  in the range of  $w \lesssim 1.6$ ; in general, the slope  $d\delta_c/dw$  depends on the value of  $\lambda_g$ .

Thus the SCBA result for the average superconducting propagator reads, in the infrared limit  $ql, \omega\tau \ll 1$ :

$$L_\omega(q) = \frac{\lambda_g}{v} \frac{1}{\delta_{\text{SCBA}} + 2[(ql)^2 + 2|\omega|\tau]^{2\lambda_g}}, \quad (16)$$

where  $\delta_{\text{SCBA}} = \delta_0 - \delta_c$  is the distance to the critical point determined within SCBA. Note that the primary effect of fluctuations in  $1/\lambda_*(\mathbf{r})$  is to strengthen a tendency to superconducting instability, which occurs now at some positive  $\delta_0 = \delta_c(w)$ .

To check the above results, we evaluate the same DoS via exact diagonalization (ED) of the discretized operator in Eq. (13), with the lattice constant equal to the mean free path  $l$ . For disorder, we choose correlated Gaussian distribution with correlation function

$$\langle u(\mathbf{r})u(0) \rangle = \frac{\Lambda}{2\pi} K_0(r/b) \quad (17)$$

at long distances  $r \gg l$ .

We discuss here the case of short-range correlations,  $b = 0.25$ . The resulting  $\nu(\epsilon)$  in a broad energy range is shown in Fig. 1a. We are mainly interested in the properties of the spectrum at energies at and below the spectrum edge of an ideal ( $w = 0$ ) system. The results for  $\rho(E)$  found from ED are shown in the main panel of Fig. 1a with dots for several values of disorder for square lattice of linear size  $L = 161$  with periodic boundary conditions. Apparently, the SCBA describes the exact DoS well for large enough energy  $E \gtrsim E_*(w)$  for all disorder strengths  $w$ . The same is true for smallest disorder  $w = 0.4$  in the whole range of energies: the effect of disorder reduces to the shift of the spectrum edge by  $-\delta_c$ , see Fig. 1a.

However, at slightly stronger disorder,  $w = 0.8$ , an enhancement (with respect to SCBA result) of the DoS at negative  $E$  is already seen; the same feature becomes more evident at larger disorder,  $w = 1.2 - 1.6$ . Functional form of this tail fits well by simple exponential dependence

$$\ln \rho(E) = C_1(w)E - C_0(w). \quad (18)$$

Parameter  $C_1$  as function of disorder strength  $w$  is shown in Fig. 1b. Exponential form (18) of the DoS will play a crucial role in our analysis below. Before proceeding, let us stress that the fact that the left tail of the DoS  $\rho(E)$  extends to arbitrary large negative  $E$  is related to the assumption of Gaussianity of  $u(\mathbf{r})$ . Due to the constraint, mentioned after Eq. (10), the Gaussian approximation fails for  $E \approx E_{\min} = -1 - \delta_0$  and a sharp band edge should be present at  $E = E_{\min}$  in any realistic model for  $u(\mathbf{r})$ . This is not a problem as there are still plenty of states for which the Gaussian approximation is valid.

In order to characterize the wavefunctions in various parts of the spectrum, we calculate the inverse participation ratio  $P_2 = \langle \sum_r \psi^4(r) \rangle$  (averaging over disorder realizations is implied) as function of the system area  $S = L^2$  and energy  $E$  at several  $w$ . Generally, one expects this scaling to be of the power-law form  $P_2(S \rightarrow \infty) = S^{-\mu}$  with  $\mu$  distinguishing between metallic ( $\mu = 1$ ), insulating ( $\mu = 0$ ) or fractal (anything in between) behavior of the wavefunctions. Fig. 1c illustrates that the states become much less localized with increase of  $E$ .

Our problem belongs to a class of problems with deterministic power-law hopping and on-site disorder [26–28], see a recent review [29]. The data discussed above indicate that the eigenfunction, corresponding to the lowest eigenvalue of the operator defined in Eq. (13), undergoes a localization transition that happens with increase of the disorder. Similar transition was studied earlier in [30–33] for other power-law-tunneling models with long-range tunneling amplitude decaying as  $r^{-\beta}$  and on-site disorder in 1D and 2D cases; see also recent papers [34–36]. Although it is expected that all states (that is, bulk states together with the edge one) are localized in thermodynamic limit at  $w > w_c$  and  $d = 2$  in such a system [36], we will make use of the fact that localization length of the excited states with sufficiently large  $E$  becomes long, as demonstrated in Fig. 1c.

Perturbative result about the absence of localization of the edge modes at *weak disorder* follows then from simple power-counting arguments provided in Ref. [31]. In our model real-space hopping

$\sim r^{-\beta}$  originates from non-analytic behavior of the kernel given in Eq. (7), thus  $\beta = 2 + 4\lambda_g$  in our case. More precisely, in Eq. (13) we have (at small  $\lambda_g$ ):

$$\Pi_0(0, \mathbf{r}) \approx -\frac{4\lambda_g}{\pi l^2} |\mathbf{r}/l|^{-\beta} \tag{19}$$

at  $|\mathbf{r}| \gg l$ . For 2D space, the arguments of Ref. [31] are valid under the condition  $2 < \beta < 3$ , thus the above inequality translates to  $0 < \lambda_g < 1/4$ .

With increase of disorder  $w$  the edge localization transition occurs, leading to appearance of localized eigenstates in the Lifschitz tail. In the present paper, we do not aim to study this specific transition in details. Our analysis in what follows will rely on the appearance of the well-defined exponential tail of the spectrum, with localized eigenstates, at super-critical disorder  $w > w_c(\lambda_g)$ . For  $\lambda_g \geq 1/4$ , localized states in the tail appear at any disorder and  $w_c = 0$ . At  $\lambda_g \rightarrow 1/4 - 0$ , critical disorder strength  $w_c$  vanishes continuously, see Ref. [31,33].

The papers [37,38] predict for this type of problems (where usual smooth solution for Lifschitz tail does not exist) existence of a Gaussian tail in the DoS,  $\ln \rho(E) \propto -E^2$ , for *arbitrary weak* disorder. This refers to the usual Schrödinger equation with random potential in high dimensions  $d > 4$  [37], and to systems with a power-law quasiparticle dispersion [38] of the type we consider at  $\lambda_g < d/8$ . Our numerical data (not shown) provide signatures of existence of this kind of states at weak disorder, although with extremely low values of DoS, much smaller than in a simple exponential tail shown in Fig. 1a for a super-critical disorder.

To conclude this Section, we emphasize again the dependence of the key parameter  $w = \Lambda b^2/l^2$  on both spatial fluctuations of Cooper constant (parameters  $\Lambda$  and  $b$ ) and on electronic mean free path  $l$ . In brief,  $\delta\lambda(\mathbf{r})$  fluctuations are more efficient when elastic scattering is strong.

### 3. Localized superconducting islands

We have found in Section 2 that eigenvalue spectrum for static superconducting fluctuations  $\Delta(\mathbf{r})$ , as determined by Eq. (11) at  $\omega = 0$ , is unbounded from below once disorder parameter is super-critical,  $w > w_c$ . According to Eq. (12), it leads to instability of all fluctuation modes with eigenvalues  $E_n < -\delta_0$ . Number of these (linearly) unstable modes grows fast upon increase of average Cooper attraction  $\bar{\lambda}$ . The amplitudes of these modes become finite upon account of nonlinear terms in the action, so one finds emergent superconducting ‘islands’ immersed in a normal metal.

Thus our strategy is, first, to study the properties of localized islands of superconductivity, and in particular dynamics of the order parameter phases  $\varphi_i(t)$  associated with those islands. Second, we will account for the interaction between phases of different islands. Such interaction comes about due to nonlinear coupling between localized and delocalized eigenmodes of the linear problem, which are defined by Eq. (13). Then the coupling between phases  $\varphi_n$  and  $\varphi_m$  of different localized modes is mediated by the propagator of delocalized modes, Eq. (16).

#### 3.1. Effective single-island action and its parameters

Individual localized modes are described by order parameters  $\Delta_i(\mathbf{r}, t) = a_i(t)\psi_i(\mathbf{r})$  where  $\psi_i(\mathbf{r})$  are normalized eigenfunctions of the linear problem (11), and  $a_i(t)$  are time-dependent complex amplitudes. The imaginary-time action  $S[a(t)]$  in terms of the amplitude  $a_i(t)$  is:

$$S = \nu \left[ \int dt \left( \frac{\alpha_i}{\lambda_g} |a_i|^2 + \frac{B_i}{2} |a_i|^4 \right) + \int \frac{d\omega}{2\pi} \Gamma_i|\omega| |a_i^{(\omega)}|^2 \right], \tag{20}$$

where  $a_i^{(\omega)}$  is the Fourier-transformed  $a_i(t)$ . Here  $\alpha_i = E_i + \delta_0$ , so all modes with negative  $\alpha_i$  are linearly unstable and the account of quartic term is mandatory; we discuss the vertex  $B_i$  a bit later. Last term in  $S[a(t)]$  accounts for damping of superconducting fluctuations in spirit of time-dependent Ginzburg–Landau (TDGL) theory. It is non-local in the imaginary-time representation, so we prefer to present it in the frequency domain. Note that under the assumed condition that superconducting islands cover small portion of system area, such a dissipative term is natural,

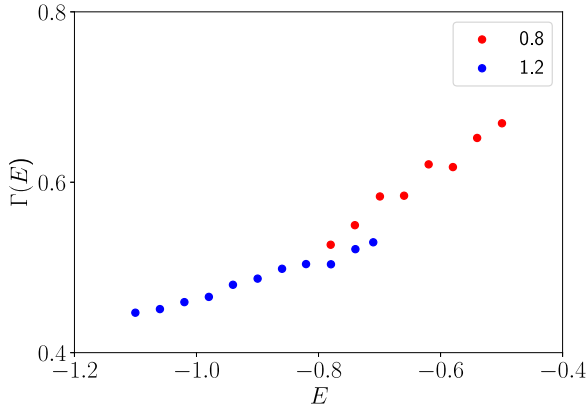


**Fig. 2.** The coefficient  $\Gamma(E)$  in Eq. (21) for two disorder values  $w = 0.8$  and  $w = 1.2$ , as shown in legend.

as dissipation is provided by gapless electrons in surrounding metal. Within usual TDGL theory operating at  $T > 0$ , the coefficient  $\Gamma \sim 1/T$  and seems to diverge in the  $T = 0$  limit. Indeed it is the case in the standard scaling theory, Ref. [39]. The crucial point of our present analysis is that we deal here with *localized* superconducting fluctuations, and the presence of finite localization length  $L_i$  corresponding to an eigenmode  $\psi_i(\mathbf{r})$ , leads also to a finite value of the kinetic constant  $\Gamma_i \sim L_i^2/D$ , i.e. it is given by electron diffusion time through the size of the corresponding superconducting eigenmode. The same estimate was obtained in Ref. [8] by a different method and for somewhat different formulation of the problem.

Quantitatively, the value of  $\Gamma_i$  can be found by the analysis of the  $\omega$  - dependence of an eigenvalue  $E_i(\omega)$  of the general linear operator defined by Eqs. (7), (11) in the range of small  $\omega \ll D/L_i^2$ . Indeed, at small  $\omega$  the major part of this  $\omega$ - dependence can be obtained by a first-order perturbation theory over  $\omega$ , without modification of the eigenstate  $\psi_i(\mathbf{r})$ . It leads then to linear in  $|\omega|$  correction to the eigenvalues

$$E_i(\omega) = E_i(0) + \Gamma_i|\omega| \quad (21)$$

which leads to the last term of the action (20). The coefficient  $\Gamma_i$  depends on energy  $E_i$  and disorder  $w$ . Illustrative examples of such a dependence are shown in Fig. 2 for two different strengths of disorder.

Now we turn to the estimates for the quartic vertex  $B_i$ . Again, finite localization length  $L_i$  leads to a finite value of  $B_i$  even in the  $T = 0$  limit, contrary to usual results [39]. Simple dimension estimates indicate that  $B_i \sim L_i^2/D^2$ . For accurate derivation of  $B_i$ , we start from general expression for the quartic term in the action as functional of slowly varying order parameter field  $\Delta(\mathbf{r}, t)$ ,

$$S_4[\Delta(\mathbf{r}, t)] = \int dt F_4(\Delta(\mathbf{r}, t)), \quad (22)$$

where quartic part of the free energy  $F_4(\Delta)$  acquires the form (for time-independent  $\Delta(\mathbf{r})$ ):

$$F_4(\Delta) = \frac{v}{2} \int \prod_{i=1}^4 d^2 r_i \Delta(\mathbf{r}_1) \Delta^*(\mathbf{r}_2) \Delta(\mathbf{r}_3) \Delta^*(\mathbf{r}_4) B_4(\{\mathbf{r}_i\}) \quad (23)$$

with (compare with Eq. (15) in Ref. [40]):

$$\begin{aligned} B_4(\{\mathbf{r}_i\}) &= \pi T \sum_{\epsilon} \prod_{k=1}^4 \frac{w_k(\epsilon)}{|\epsilon| + \frac{1}{2}D(-i\partial_k)^2} \delta(\mathbf{r}_1 - \mathbf{r}_2) \delta(\mathbf{r}_1 - \mathbf{r}_3) \delta(\mathbf{r}_1 - \mathbf{r}_4) H_{\epsilon}(-i\partial_1, -i\partial_2, -i\partial_3, -i\partial_4) \\ &= \pi T \sum_{\epsilon} \prod_{k=1}^4 \int \frac{(d^2 \mathbf{p}_k) w_k(\epsilon)}{|\epsilon| + D p_k^2 / 2} \delta(\mathbf{p}_1 + \mathbf{p}_3 - \mathbf{p}_2 - \mathbf{p}_4) e^{i\mathbf{p}_1 \mathbf{r}_1 + i\mathbf{p}_3 \mathbf{r}_3 - i\mathbf{p}_2 \mathbf{r}_2 - i\mathbf{p}_4 \mathbf{r}_4} H_{\epsilon}(\mathbf{p}_1, \mathbf{p}_2, \mathbf{p}_3, \mathbf{p}_4). \end{aligned} \quad (24)$$



where ‘screening factors’  $w_k(\epsilon) \equiv w_{\mathbf{p}_k}(\epsilon)$  are given by Eqs. (4) and Hikami box reads

$$H_\epsilon(\{\mathbf{p}_i\}) = |\epsilon| + \frac{D}{8} [(\mathbf{p}_1 - \mathbf{p}_3)^2 + (\mathbf{p}_2 - \mathbf{p}_4)^2]. \tag{25}$$

The order parameter  $\Delta(\mathbf{r})$  in this expression should be written in terms of the eigenstates  $\psi_n(\mathbf{r})$  of quadratic part of the action  $S_2$ :  $\Delta(\mathbf{r}) = \sum_n a_n \psi_n(\mathbf{r})$ . As a result, a quartic mode-coupling between  $a_n$  arises. We will first discuss the contributions where all eigenstate indices are equal:  $F_4^{(1)} = \frac{\nu}{2} \sum_n |a_n|^4 B_n$ . It is optimal to rewrite  $B_n$  as follows:

$$B_n = \pi T \sum_\epsilon \int d^2r [|\epsilon| |G_{n,\epsilon}|^4(\mathbf{r}) + \frac{D}{2} (|G_{n,\epsilon}|^2(\mathbf{r}) \text{Re } G_{n,\epsilon}(\mathbf{r}) F_{n,\epsilon}^*(\mathbf{r}) + \text{Re } \mathbf{H}_{n,\epsilon}^2(\mathbf{r}) (G_{n,\epsilon}^*)^2(\mathbf{r}))] \tag{26}$$

with

$$G_{n,\epsilon}(\mathbf{r}) = \sum_p \frac{e^{i\mathbf{p}\mathbf{r}}}{|\epsilon| + \frac{1}{2} D p^2} w_p(\epsilon) \Psi_n(\mathbf{p}), \tag{27}$$

$$\mathbf{H}_{n,\epsilon}(\mathbf{r}) = \sum_p \frac{e^{i\mathbf{p}\mathbf{r}} i\mathbf{p}}{|\epsilon| + \frac{1}{2} D p^2} w_p(\epsilon) \Psi_n(\mathbf{p}),$$

$$F_{n,\epsilon}(\mathbf{r}) = \sum_p \frac{e^{i\mathbf{p}\mathbf{r}} p^2}{|\epsilon| + \frac{1}{2} D p^2} w_p(\epsilon) \Psi_n(\mathbf{p}).$$

where factors  $w_q(\epsilon)$  are defined in Eq. (4) and  $\Psi_n(\mathbf{p})$  stay for Fourier-transform of eigenstates  $\psi_n(\mathbf{r})$ . Below we evaluate integrals in Eqs. (27) at  $T = 0$  for eigenfunctions  $\psi_n(\mathbf{r})$  localized at relatively short  $L_n$ . These integrals are dominated by  $\epsilon \sim D/L_n^2$  and  $p \sim 1/L_n$ , thus the factor  $w_q(\epsilon) \approx 1/\cosh(2\lambda_g \ln(L_n/l))$ . For the final result of integration in Eq. (26) we find an estimate

$$B_n \sim \frac{L_n^2}{D^2 \cosh^4(2\lambda_g \ln \frac{L_n}{l})}, \tag{28}$$

which differs from the dimensional estimate  $B_n \sim L_n^2/D^2$  (provided originally in Ref. [8]) by  $\cosh^4(\dots)$  factor only. We do not expect this modification to be significant due to smallness of  $\lambda_g$  and not very large ratio  $L_n/l$  for relevant localized eigenstates  $\psi_n(\mathbf{r})$ .

### 3.2. Relevant time-scales of localized superconducting modes

At large positive  $\alpha_i = E_i + \delta_0$  typical frequency of eigenmode is

$$\omega_i \sim \alpha_i/\lambda_g \Gamma_i \sim \alpha_i D/\lambda_g L_i^2. \tag{29}$$

This estimate comes from the comparison between 1st and 3rd terms in the action (20). At large negative  $\alpha_i$  the energy is minimized by  $|a_i|^2 = -\alpha_i/\lambda_g B_i \sim |\alpha_i| D^2/\lambda_g L_i^2$  and two different fluctuation modes appear. Longitudinal mode corresponds to variation of  $|a_i|$ , and its frequency is  $\omega_i \sim |\alpha_i| D/\lambda_g L_i^2 = D|E_i + \delta_0|/\lambda_g L_i^2$ . We will see now that at large enough  $|\alpha_i|$ , the typical timescale of the transverse (phase rotation) mode become much longer. We define local phase  $\varphi_i(t)$  via relation  $a_i = |a_i| e^{i\varphi_i(t)}$  and obtain phase-dependent action in the frequency domain

$$S[\varphi] = \frac{\nu}{\lambda_g} \int d\omega |\omega| \Gamma_i |a_i|^2 (\exp(i\varphi))_\omega (\exp(-i\varphi))_{-\omega} \tag{30}$$

$$= \tilde{c} \frac{g}{4\pi \lambda_g} \int d\omega |\omega| (\bar{\lambda} - E_i) (\exp(i\varphi))_\omega (\exp(-i\varphi))_{-\omega} \tag{31}$$

In Eq. (31) we substituted the estimates for  $\Gamma_i$  and  $B_i$  together with the relation  $4\pi\nu D = g$  and  $\tilde{c}$  is some factor  $\sim 1$ . Equivalent action in the time domain is

$$S[\varphi(t)] = \frac{G_i}{2\pi^2} \int dt_1 dt_2 \frac{\sin^2[(\varphi(t_1) - \varphi(t_2))/2]}{(t_1 - t_2)^2}, \quad (32)$$

where

$$G_i = \frac{g\tilde{c}}{\lambda_g} |E_i + \delta_0| = -\frac{g\tilde{c}}{\lambda_g} (E_i + \delta_0). \quad (33)$$

The action (32) is similar to the one defined in Eq. (3) of Ref. [6], where phase dynamics of artificially prepared superconducting islands was studied; the constant  $G_i$  plays the role of the effective Andreev conductance measured in units of  $4e^2/2\pi\hbar$ .

Below we consider islands with large values of  $G_i$ , which definitely exist due to large parameter  $g \gg 1$ . For such islands, autocorrelation function  $C_i(t) = \langle \cos(\varphi(0) - \varphi(t)) \rangle$  decreases logarithmically [6] at moderate times  $t \leq t_i$ , while at the longest time scales  $C(t) \propto G_i^{-1}(t_i/t)^2$ , where correlation time of the  $i$ th island

$$t_i \approx \omega_i^{-1} \exp(G_i/2). \quad (34)$$

Below we focus on exponential dependence of  $t_i$  on the parameters of islands entering (34) via  $G_i$ , and neglect variations of prefactors  $\omega_i = |\alpha_i|D/\lambda_g L_i^2$ , replacing them by some typical frequency scale

$$\omega_{\text{typ}} = \frac{\alpha_{\text{typ}} D}{\lambda_g L_{\text{loc}}^2}. \quad (35)$$

Here  $\alpha_{\text{typ}}$  is the typical value of  $|E_i + \delta_0|$  for relevant islands, and  $L_{\text{loc}}$  is their typical localization length. Exponential relation (34) together with exponential form of the DoS of localized states, Eq. (18), lead to the power-law tail in the probability distribution for the phase relaxation rates  $\gamma_i = 1/t_i$ . Normalizing this probability distribution per unit area, and making use of Eqs. (18), (33), (34), (35) we find, in the range  $\gamma_i < \omega_{\text{typ}}$ :

$$P_0(\gamma) d\gamma \approx \frac{p_0}{L_{\text{loc}}^2} \left( \frac{\gamma}{\omega_{\text{typ}}} \right)^{\eta_0} \frac{d\gamma}{\omega_{\text{typ}}} = \frac{p_0 \lambda_g}{D \alpha_{\text{typ}}} \left( \frac{\gamma}{\omega_{\text{typ}}} \right)^{\eta_0} d\gamma, \quad (36)$$

using  $L_{\text{loc}}^2$  for typical area of relevant islands. Here

$$\eta_0 = \frac{2C_1(w)\lambda_g}{\tilde{c}g} - 1, \quad (37)$$

$$p_0(\delta_0) = 2 \frac{\lambda_g}{\tilde{c}g} e^{-C_0(w) - C_1(w)\delta_0} \quad (38)$$

with  $p_0 \ll 1$  for the probability to find a superconducting island with phase relaxation rate  $\gamma \sim \omega_{\text{typ}}$  within an area  $\sim L_{\text{loc}}^2$ . This probability is exponentially low in the normal metal state, where  $C_1(w)\delta_0 \gg 1$ . Let us discuss how it is affected by variations in the main quantities describing the system. (i) Growth of average attraction  $\bar{\lambda}$  leads to decrease of  $\delta_0$  (see Eq. (10)) and thus to sharp increase of the density of islands with slow relaxation rates. (ii) Increase of the disorder parameter  $w$  diminishes the power-law exponent  $\eta_0$ , see Fig. 1c. (iii) Increase of the film conductance  $g$  at fixed value of  $w$  would result in decrease of  $\eta_0$ . However, since  $w \propto 1/l^2 \propto 1/g^2$  (see discussion in the end of Section 2) and  $C_1(w)$  grows fast with decrease of  $w$ , the increase of  $g$  translates to increase of  $\eta_0$ .

Exponent  $\eta_0$  plays crucial role in the further analysis. The (extended) critical domain near q-SMT is characterized by  $\eta_0 \leq 1$ , while at  $\eta_0 \gg 1$  superconducting islands are of little importance for the macroscopic properties of the film. Note that average correlation time  $\langle 1/\gamma \rangle$  is finite for  $\eta_0 > 0$ , while its variance diverges for all  $\eta_0 \leq 1$ . We will now consider the interaction between different islands and show that this interaction leads to renormalization of  $\eta_0$  downwards.

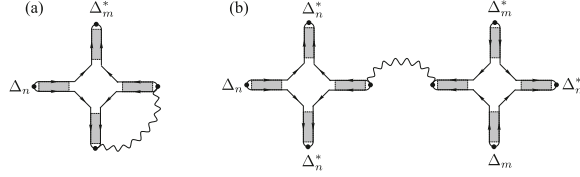


**Fig. 3.** First-order (a) and second-order (b) diagrams for the coupling between phases  $\varphi_{n,m}$  of distant islands. Wavy lines stay for the propagator  $L_\omega(q)$ .

### 3.3. Inter-island coupling

Now we proceed with the calculation of the interaction between order parameters of distant localized islands  $m$  and  $n$ , both unstable with respect to appearance of nonzero amplitudes of the order parameter,  $a_n = |a_n|e^{i\varphi_n}$  and  $a_m = |a_m|e^{i\varphi_m}$ . Within the quadratic approximation defined by the action  $S_2(\Delta)$ , Eq. (1), these islands do not interact by construction:  $\psi_n(\mathbf{r})$  are the eigenfunctions of the corresponding linear operator, Eqs. (11), (13). To derive the Josephson-type coupling  $F_{\text{int}}(\varphi_n - \varphi_m)$  we need to account for non-Gaussian contributions to the action, so our starting point is given by Eqs. (23), (24).

The simplest relevant diagram is shown in Fig. 3a, it contains one nonlinear vertex  $B_4$  and one loop with dynamic superconducting propagator  $L_\omega(q)$ , see Eq. (16). We choose here  $\Delta_n = a_n\psi_n(\mathbf{r})$  and  $\Delta_m = a_m\psi_m(\mathbf{r})$  describing  $n$ th and  $m$ th localized islands, while summation over two extended modes is expressed via their propagator  $L_\omega(q)$ . For time-independent phases  $\varphi_{n,m}$ , the result of integration over frequency and momenta in the loop shown in Fig. 3a can be written in the form of the interaction energy:

$$E_{\text{int},1}^{n,m} = -\tilde{J}_{nm} \cos(\varphi_m - \varphi_n), \quad (39)$$

where matrix elements  $\tilde{J}_{nm} = \tilde{J}(R_{nm})$  depend on the distance  $R_{nm}$  between centers of localized eigenstates  $\psi_{n,m}(\mathbf{r})$ ; this distance is well defined as long as  $R_{nm} \gg L_{\text{loc}}$ . An important result of the calculation is that zero Fourier-harmonic of this interaction,  $\tilde{J}(Q=0) = \sum_{\mathbf{R}} \tilde{J}(\mathbf{R})$ , does not contain any singularity when the parameter  $\delta_{\text{SCBA}}$  entering Eq. (16) approaches zero. In other terms, the integral defining  $\tilde{J}(Q=0)$  is determined by the ultraviolet region (large  $q, \omega$ ) insensitive to the proximity to a bulk superconductor-metal transition.

Below we consider another source of long-range interaction, which does contain singular enhancement at  $\delta_{\text{SCBA}} \rightarrow 0$  and thus is the key driving force which establishes long-range coherence between well-separated islands.

The most long-range contribution to the pair-wise interaction energy between phases  $\varphi_m$  and  $\varphi_n$  appears in the second order of perturbation theory over nonlinear vertex  $B_4$  and contain one superconducting propagator  $L_\omega(\mathbf{R})$ , with its Fourier representation in Eq. (16), see Fig. 3b. In terms of the interaction contribution to the action  $S_{\text{int}}$  we find, using Eqs. (22), (23), (24):

$$S_{\text{int}} = -\frac{v^2}{4} \int dt dt' \int \Pi_{i=1}^4 d^2 r_i \Pi_{i=1}^4 d^2 r'_i B_4(\{\mathbf{r}_i\}) \Delta_n(\mathbf{r}_1, t) \Delta_n^*(\mathbf{r}_2, t) \Delta_n(\mathbf{r}_3, t) \times B_4(\{\mathbf{r}'_i\}) \Delta_m^*(\mathbf{r}'_1, t') \Delta_m(\mathbf{r}'_2, t') \Delta_m^*(\mathbf{r}'_3, t') \times L(\mathbf{r}_4 - \mathbf{r}'_4, t - t'), \quad (40)$$

where propagator  $L(\mathbf{r}_4 - \mathbf{r}'_4, t - t') = \langle \Delta(\mathbf{r}_4, t) \Delta^*(\mathbf{r}'_4, t') \rangle$  describes quantum fluctuations of delocalized modes.  $\Delta_n(\mathbf{r}) = a_n\psi_n(\mathbf{r})$  and  $\Delta_m(\mathbf{r}') = a_m\psi_m(\mathbf{r}')$  correspond to the order parameters of superconducting islands  $n, m$ . We assume the islands to be localized around their centers located at  $\mathbf{R}_n$  and  $\mathbf{R}_m$ , and define  $\psi_n(\mathbf{r}) = \tilde{\psi}_n(\mathbf{r} - \mathbf{R}_n)$  and  $\psi_m(\mathbf{r}') = \tilde{\psi}_m(\mathbf{r}' - \mathbf{R}_m)$ . Here  $\tilde{\psi}(\tilde{\mathbf{r}})$  functions are localized around zeros of their arguments within small lengths  $L_{n,m} \ll |\mathbf{R}_n - \mathbf{R}_m|$ . It is convenient now to use space-time Fourier representation in terms of  $L_\omega(q)$  for the propagator  $L(\mathbf{r}_4 - \mathbf{r}'_4, t - t')$ ,

in order to split the whole multiple integral in Eq. (40) into two factorized parts:

$$\begin{aligned}
 -S_{\text{int}}[\varphi_n(t), \varphi_m(t)] &= \frac{\nu^2}{4} |\alpha_n|^3 |\alpha_m|^3 \\
 &\times \int \frac{d\omega}{2\pi} \frac{d^2q}{(2\pi)^2} \text{Re} [s_n(\omega) s_m^*(\omega) A_n A_m^*] L_\omega(q) e^{i\mathbf{q}(\mathbf{R}_n - \mathbf{R}_m)},
 \end{aligned}
 \tag{41}$$

where  $s_{n,m}(\omega)$  stay for the Fourier-transforms of the time-domain functions  $e^{i\varphi_{n,m}(t)}$ . Coefficients  $A_n$  ( $A_m$ ) contain 4 integrals over space coordinates  $\mathbf{r}_k$  ( $\mathbf{r}'_k$ ). Consider the structure of  $A_n$  more closely ( $A_m$  is completely analogous):

$$A_n = \Pi_{i=1}^4 \int d^2r_i B_4(\{\mathbf{r}_i\}) \tilde{\psi}_n(\mathbf{r}_1) \tilde{\psi}_n^*(\mathbf{r}_2) \tilde{\psi}_n(\mathbf{r}_3) e^{i\mathbf{q}\mathbf{r}_4}.
 \tag{42}$$

The major dependence on  $q$  in the final expression (41) comes from  $L_\omega(q)$ , and factors  $A_n, A_m$  can be considered as  $q$ -independent. Then the representation (24) for  $B_4(\{\mathbf{r}_i\})$  can be used to rewrite  $A_n$  in the form similar to Eq. (26) for  $B_n$ . At zero temperature:

$$A_n = \int_0^{1/\tau} \frac{(\epsilon\tau)^{\lambda_g} d\epsilon}{\epsilon} \int d^2r \left[ \epsilon \tilde{G}_{n,\epsilon}^3(\mathbf{r}) + \frac{D}{4} \tilde{G}_{n,\epsilon}^*(\mathbf{r}) \tilde{\mathbf{H}}_{n,\epsilon}^2(\mathbf{r}) + \frac{D}{8} \left( 2|\tilde{G}_{n,\epsilon}|^2(\mathbf{r}) \tilde{F}_{n,\epsilon}(\mathbf{r}) + \tilde{G}_{n,\epsilon}^2(\mathbf{r}) \tilde{F}_{n,\epsilon}^*(\mathbf{r}) \right) \right],
 \tag{43}$$

where functions  $\tilde{G}, \tilde{F}, \tilde{\mathbf{H}}$  are defined like functions  $G, F, \mathbf{H}$  in Eqs. (27), but with the replacements  $\Psi_n(\mathbf{p}) \rightarrow \tilde{\Psi}_n(\mathbf{p})$ . Screening factors  $w_p(\epsilon) = 1/\cosh(2\lambda_g \ln(pl))$ , entering integrals in (27), will be set to unity, since relevant  $p \sim 1/L_n$  are relatively large and  $\lambda_g \ll 1$ . The largest contribution to  $A_n$  comes from the last two terms in (43), which contain  $\tilde{G}^2 \tilde{F}$  products. Functions  $\tilde{G}(\mathbf{r})$  and  $\tilde{F}(\mathbf{r})$  are localized within the range about  $L_n$  around their maxima, while their amplitudes at maximum can be estimated as  $L_n/D$  and  $1/(L_n D)$  correspondingly. The energy integral in Eq. (43) produces extra factor  $1/\lambda_g$ . As a result, we come to the estimate  $A_n \sim \frac{l_n^3}{\lambda_g D^2}$ .

Taking also into account  $|\alpha_n| \approx \sqrt{|\alpha_n|/\lambda_g D/L_n}$ , we find eventually

$$S_{\text{int}}[\varphi_n, \varphi_m] = - \int \frac{d\omega}{2\pi} s_n(\omega) s_m^*(\omega) J_{nm}^{(\omega)}(\mathbf{R}_{nm})
 \tag{44}$$

where (see Eq. (16))

$$J_{nm}^{(\omega)}(\mathbf{r}) \approx \frac{g}{\lambda_g^4} |\alpha_n|^{3/2} |\alpha_m|^{3/2} \int \frac{D(d^2q/(2\pi)^2) e^{i\mathbf{q}\mathbf{r}}}{\delta_{\text{SCBA}} + 2[(ql)^2 + 2|\omega|\tau]^{2\lambda_g}}
 \tag{45}$$

Note that localization lengths  $L_{n,m}$  cancel out from Eq. (45), once we put  $\cosh(2\lambda_g \ln(L_n/l)) \approx 1$ . Eqs. (44), (45) define interaction action for two superconducting islands.

Generally, this action cannot be reduced to the interaction Hamiltonian, due to frequency dispersion entering  $J_{nm}^{(\omega)}(\mathbf{r})$ . However, if one is interested in *relatively slow* fluctuations of phases  $\varphi_{n,m}(t)$ , then  $s_{n,m}(\omega) \approx e^{i\varphi_{n,m}} \delta(\omega)$  and one may use, instead of the action (44), the Hamiltonian of the form of Eq. (39), but with matrix elements

$$J_{nm}(\mathbf{R}_{nm}) = A_{nm} \int \frac{d^2q}{(2\pi)^2} \frac{e^{i\mathbf{q}\mathbf{R}_{nm}}}{\delta_{\text{SCBA}} + 2(ql)^{4\lambda_g}},
 \tag{46}$$

with

$$A_{nm} \propto \frac{\nu D^2}{\lambda_g^4} |\alpha_n|^{3/2} |\alpha_m|^{3/2},
 \tag{47}$$

where we omitted numerical factor of the order of unity. Below we will assume that reduction of the full dynamic problem (44) to the Hamiltonian with matrix elements (46) is a good approximation. We checked this assumption in the Supplement S1, where analysis of the two-island dynamics with full interaction  $J_{nm}^{(\omega)}(\mathbf{r})$  was performed.

For the interaction strength in real space we obtain, after integration in Eq. (46):

$$J_{nm}(\mathbf{r}) \approx \frac{A_{nm}}{\pi} \frac{\lambda_g(r/l)^{4\lambda_g}}{r^2 [1 + (\delta_{SCBA}/2)(r/l)^{4\lambda_g}]^2}. \quad (48)$$

Note the presence of long (at small  $\delta_{SCBA}$ ) spatial scale  $r^* = l\delta_{SCBA}^{-1/4\lambda_g}$ . Function  $J_{nm}(r) \sim 1/r^{2-4\lambda_g}$  does not depend on  $\delta_{SCBA}$  for  $r \leq r^*$ , and it scales as  $J_{nm}(r) \sim \delta_{SCBA}^{-2} \times 1/r^{2+4\lambda_g}$  at  $r \geq r^*$ . Major contribution to the integral  $\mathcal{J}_{nm}(0) = \int J(r)d^2r \sim A_{nm}/\delta_{SCBA}$  comes from  $r \sim r^*$ .

Below we assume that typical interacting pairs of islands are separated by a large distance  $r_{nm} \geq r^*$ . In result, the total interaction Hamiltonian reads

$$H_{\text{int}} = - \sum_{nm} J_{nm} \cos(\varphi_n - \varphi_m), \quad (49)$$

where coupling matrix elements

$$J_{nm} = \frac{C_{nm}}{|\mathbf{R}_n - \mathbf{R}_m|/l}^\beta \quad (50)$$

and the coefficients  $C_{nm}$  are:

$$C_{nm} = \frac{4\lambda_g A_{nm}}{\pi \delta_{SCBA}^2 l^2} \propto \frac{\nu v_F^2}{\lambda_g^2 \delta_{SCBA}^2} |\alpha_n|^{3/2} |\alpha_m|^{3/2}, \quad (51)$$

where we omitted numerical factor of order unity. To obtain last form of  $C_{nm}$ , we used relation  $D = \nu l/2$ ; for isotropic model of 2D metal,  $\nu v_F^2 = \epsilon_F/\pi$ . The constants  $C_{nm}$  contain product of large factors  $\epsilon_F$  and  $\delta_{SCBA}^{-2}$  by small  $\sim \alpha_{n,m}^3$ . It is assumed that typical distance  $R_{nm} = |\mathbf{R}_n - \mathbf{R}_m|$  is much longer than  $l$ .

Our analysis below is based upon the single-island action (32) and the interaction Hamiltonian (49).

## 4. Effect of interaction between islands at $T = 0$ : strong disorder RG

### 4.1. General approach and RG equations

Results of Section 2 demonstrate crucial property of the q-SMT in presence of sufficiently strong fluctuations  $\delta\lambda(\mathbf{r})$ : locally superconducting regions (islands) appears at random locations and are localized on typical length  $L_{\text{loc}}$  which is much shorter than typical distance between islands

$$L_0 \sim \frac{L_{\text{loc}}}{\sqrt{p_0}} \gg L_{\text{loc}}, \quad (52)$$

where  $p_0$  is defined in Eq. (38). Far from the SMT, in the normal state, the density  $n_{\text{isl}} = 1/L_0^2$  is too low for interaction terms, Eq. (49) to be relevant, thus phases of individual islands fluctuate independently. With increase of average attraction and decrease of  $\delta_0$ , the density  $n_{\text{isl}}$  grows, as well as the probability that some islands occur to be close enough to interact strongly. For each pair of islands,  $n$  and  $m$ , the strength of this interaction  $J_{nm}$ , defined in Eq. (50), is to be compared to the relaxation rates of the same islands  $\gamma_n, \gamma_m$ . We are interested especially in the range of parameters where the key exponent  $\eta_0$  satisfies  $0 < \eta_0 \leq 1$ , thus individual decay rates  $\gamma_n$  are distributed widely in the small- $\gamma$  domain.

Quantum fluctuations of phases  $\varphi_n(t)$  and  $\varphi_m(t)$  are mutually independent if at least one of the rates  $\gamma_n, \gamma_m$  is much larger than the coupling energy  $J_{nm}$ . If, however,  $\min(\gamma_n, \gamma_m) \ll J_{nm}$ , then dynamics of phases  $\varphi_n(t), \varphi_m(t)$  becomes correlated at the time scales longer than  $1/J_{nm}$  and phase difference  $\varphi_n(t) - \varphi_m(t)$  ceases to grow with time. In result (see Sec. S1 of the Supplemental Material for details), the joint two-island decay rate  $\gamma_{nm}$  becomes much smaller than the individual rates  $\gamma_n$  and  $\gamma_m$ :

$$\gamma_{nm} = \frac{\gamma_n \gamma_m}{J_{nm}} \quad \text{for} \quad \min(\ln(\gamma_n), \ln(\gamma_m)) < \ln(J_{nm}). \quad (53)$$

To understand Eq. (53) it is enough to notice that lowest-frequency Andreev conductance of the two-island system  $G_{nm} = G_n + G_m$ , while the relevant pre-exponential factor in the expression like Eq. (34) is given now by the timescale  $1/J_{nm}$  where interaction between islands sets in; see Eq. (94) for details.

'Fusion rule' (53) shows that interaction between different islands slows down dynamics of their phases. Eventually, under many such fusions, it can lead to the complete freezing of this dynamics, leading to macroscopic phase coherence and superconductivity. An appropriate quantitative method to describe this phenomenon is known as Strong Disorder Renormalization Group (SDRG) developed originally for one-dimensional quantum Ising model in random transverse field [17,18] and employed later on for numerous different problems, see reviews [19–21]. The SDRG method is useful when the Hamiltonian contains competing terms with random amplitudes, and one (or more) of these amplitudes is characterized by a very broad probability distribution. Precisely this property invalidates the use of mean-field approach [6,7], even in the case of long-range interactions, like proximity coupling (50). The idea of SDRG is to integrate out quantum degrees of freedom of large system sequentially, starting from the highest energy scale, and to derive stochastic evolution equations for the remaining amplitudes entering the Hamiltonian.

The most similar physical problem treated by this kind of approach [41–44], refers to the q-SMT in quasi-one-dimensional wires with strong pair-breaking. Dynamics of individual islands was considered to be of the same kind as we described above, see Eqs. (34), (53). However, in these references the proximity coupling was considered to be short-ranged (due to strong pair-breaking), and the problem was thus reduced to a nearest-neighbor coupling model. It results [41] in a multiplicative recursion relations for renormalized couplings  $J_{ij}$ , similar in its structure to the one for individual decay rates, Eq. (53). Then the whole SDRG belongs to the same universality class as random-field Ising model [17,18]. This is not the case for our problem with long-range proximity coupling (50), with  $2 < \beta < 3$ . However, SDRG scheme appropriate for our model was also developed and studied, although in somewhat different contexts [22,45]. Below we adapt to our problem the method of Ref. [22] which is a dual alternative of the one developed in Ref. [45].

We employ a 2D version of the 'primary model' defined in Ref. [22], where a problem of a quantum transverse-field Ising model with power-law exchange coupling of the type (50) was studied. Interaction between islands starts to become relevant when the magnitude of  $J_{nm}$ , Eqs. (50), (51), for typical nearest-neighbor distance  $R_{nm} \sim L_0$  becomes comparable to the typical value of island's relaxation rates  $\omega_{\text{typ}}$  defined in Eq. (35). The corresponding condition can be written, with the use of Eqs. (35), (50), (51), in the form

$$[p_0(\delta_0)]^{\beta/2} \propto \left( \frac{\delta_{\text{SCBA}}}{\alpha_{\text{typ}} g} \right)^2, \quad (54)$$

where we omitted numerical factor of order unity. Here  $\alpha_{\text{typ}}$  is the magnitude of  $|E_i + \delta_0|$  for typical relevant islands. In the further analysis we put  $\alpha_{\text{typ}} \approx 1/g$ , in order to get moderately large  $G_i$  for relevant islands, see Eq. (33). While deriving Eq. (54) we put  $(L_{\text{loc}}/l)^{4\lambda_g} \approx 1$ , as it was already done earlier.

In order to find the value of  $\delta_0$  entering Eq. (54), we need to solve Eqs. (38), (54) together. As a result, we find:

$$\delta_{\text{SCBA}} \propto \frac{1}{g^{3\beta/8}} \exp \left[ -\frac{\beta}{4}(C_0 + C_1 \delta_c) \right] \ll 1, \quad (55)$$

where we omitted numerical factor of order unity. The corresponding length-scale  $L_0$  is given by

$$L_0 \sim L_{\text{loc}} g^{3/4} \exp \left[ \frac{1}{2}(C_0 + C_1 \delta_c) \right] \gg L_{\text{loc}}. \quad (56)$$

The relation (56) determines the spatial length scale  $L_0$ , where the SDRG procedure starts in. The corresponding energy scale  $\Omega_0 = \omega_{\text{typ}}$  is defined in Eq. (35).

We now describe briefly the SDRG approach. Starting from the upper energy cutoff  $\Omega_0 \sim \omega_{\text{typ}}$  (see Eq. (35)), at any value of running RG energy scale  $\Omega \leq \Omega_0$ , we look for the largest energy parameter in the system, it is equal to  $\Omega$  by definition. It can be either the rate  $\gamma_i$  of the  $i$ th island, or

the coupling  $J_{nm}$  between  $n, m$  pair of them. In the first case,  $i$ th island is decimated, while couplings between remaining islands are left unchanged. As a result, typical area corresponding to distance between nearest remaining islands grows linearly:  $S_{nm} = S_{ni} + S_{im}$ . The same relation can be written in the form  $J_{nm}^{-2/\beta} = J_{im}^{-2/\beta} + J_{ni}^{-2/\beta}$ . Now we introduce dimensionless variable  $y = (\Omega/J)^{2/\beta} - 1$ , so it vanishes at  $J = \Omega$ . The above recursion relation for  $J_{nm}$  reads then as

$$y_{nm} = y_{ni} + y_{im} + 1. \tag{57}$$

Below we will see that actual probability distribution  $Q(y)$  becomes very broad near the q-SMT, thus the term 1 in the R.H.S. of Eq. (57) can be neglected.

If the largest energy parameter in the Hamiltonian close in its value to  $\Omega$  is some coupling  $J_{nm}$ , its decimation leads to modification of the rates  $\gamma_{n,m}$  according to Eq. (53). It is convenient to introduce logarithmic variables  $x_n = (2/\beta) \ln(\Omega/\gamma_n)$ , then the recursion relation equivalent to (53) reads as

$$x_{nm} = x_n + x_m. \tag{58}$$

Factor  $2/\beta$  in the definition of  $x_n$  variable is introduced in order to simplify the following equations, since the same factor enters the definition of  $y_n$ .

Derivation of the functional RG equations for probability densities  $P(x)$  and  $Q(y)$  corresponding to stochastic equations Eqs. (57), (58) is provided in Refs. [21,45]. We reproduce it in Supplement S2 together with some extension. The RG evolution parameter is defined by the logarithmic variable  $\tau = (2/\beta) \ln(\Omega_0/\Omega)$  which counts logarithm of average area per a cluster in the system of interacting islands with a largest energy scale  $\Omega$ . The functional RG equations allow quasi-stationary solutions of exponential form:

$$P(x, \tau) = p(\tau)e^{-p(\tau)x} \quad Q(y, \tau) = q(\tau)e^{-q(\tau)y} \tag{59}$$

if the functions  $p(\tau)$  and  $q(\tau)$  obey the system of equations

$$\frac{dp}{d\tau} = -p \cdot q, \tag{60}$$

$$\frac{dq}{d\tau} = -p \cdot q + q. \tag{61}$$

Eqs. (60), (61) are formally equivalent to the Kosterlitz RG equations [46] for 2D XY model. They differ from similar equations of the Fisher's SDRG by the presence of the last term  $q$  in (61). This term is due to trivial scaling dimension 1 of the variable  $y$ , while variable  $x$  is dimensionless.

The system of Eqs. (60), (61) possesses the first integral  $q(\tau) - p(\tau) + \ln p(\tau) = \text{Const}$  which allows to reduce it to a single equation for  $p(\tau)$ . Below we will be most interested in the vicinity of the critical point where  $p(\tau)$  is close to unity. Thus we denote  $p(\tau) = 1 + \xi(\tau)$ , keep major terms of expansion over  $\xi(\tau) \ll 1$  (we will find that  $\xi \sim \sqrt{\delta}$ ) and obtain single RG equation

$$\frac{d\xi}{d\tau} = -\frac{\xi^2}{2} + \delta, \tag{62}$$

where  $\delta \ll 1$  parametrizes the distance to the critical point. Within the same accuracy,  $q(\tau) = \xi^2/2 - \delta$ .

During the RG transformation, SC islands continuously merge, so the areal density  $n(\tau)$  of survived islands decreases according to the equation

$$\frac{dn}{d\tau} = -(p(\tau) + q(\tau))n(\tau), \tag{63}$$

which follows from the fact that at each decimation (island or bond) the number of surviving islands decreases by one. Its solution is

$$n(\tau_\Omega) = n_0 \exp\left(-\int_0^{\tau_\Omega} (p(\tau) + q(\tau)) d\tau\right), \tag{64}$$

where  $n_0 \sim L_0^{-2}$  is the initial density of islands at the starting energy scale of RG,  $\Omega_0$ .

Another important characteristic of the inhomogeneous state formed due to RG procedure is average number of islands  $N(\tau_\Omega)$  which constitute a cluster formed at the scale

$$\tau_\Omega = (2/\beta) \ln(\Omega_0/\Omega). \tag{65}$$

Contrary to  $n(\tau_\Omega)$ , this quantity is determined by the integration over the whole RG trajectory. We present necessary calculations in the Section S2 of the Supplemental Material (see also Ref. [47]). The result is given by

$$N(\tau_\Omega) = \int_0^{\tau_\Omega} p_1(\tau) d\tau, \tag{66}$$

here function  $p_1(\tau) \equiv p_1(\xi(\tau))$ , where  $p_1(\xi)$  solves Eq. (103). Explicit solutions following from Eqs. (64) and (66) will be presented below, separately for  $\delta > 0$  and  $\delta < 0$ .

#### 4.2. Metal phase: line of RG fixed points

At small  $\delta > 0$ , full solution to Eqs. (60), (61) reads:

$$p(\tau) = 1 + \sqrt{2\delta} \coth \left( \sqrt{\frac{\delta}{2}} (\tau + \tau_+) \right), \tag{67}$$

$$q(\tau) = \frac{\delta}{\sinh^2 \left( \sqrt{\frac{\delta}{2}} (\tau + \tau_+) \right)}. \tag{68}$$

Integration constant  $\tau_+$  and key parameter  $\delta$  should be determined by the matching of quasi-stationary distributions (59) to the bare distributions  $P_0(\gamma)$  (see Eq. (36)) and  $Q_0(J)$ :

$$1 + \sqrt{2\delta} \coth \left( \tau_+ \sqrt{\frac{\delta}{2}} \right) = \frac{\beta}{2} (1 + \eta_0), \tag{69}$$

$$\frac{\delta}{\sinh^2 \left( \tau_+ \sqrt{\frac{\delta}{2}} \right)} = Q_0(J \sim \Omega_0). \tag{70}$$

To derive Eq. (69), we employed the relation  $\gamma \propto \exp(-\beta x/2)$ . Right-hand sides of both Eqs. (69), (70) are of the order of unity; thus we need  $\tau_+ \sim 1$  in order that  $\delta \ll 1$  cancels out from the LHS's of these equations. Then we see that at  $\delta \ll 1$  the integration constant  $\tau_+$  is not important for the asymptotic solutions and will be ignored below.

The solution provided by Eqs. (67), (68) defines a line of fixed points parametrized by  $\delta > 0$ . In the infrared limit  $\tau \rightarrow \infty$ , we find  $p(\infty) = 1 + \sqrt{\delta/2}$ , and  $q(\tau) \approx 4\delta e^{-\sqrt{2\delta}\tau}$ . The scale  $\tau_\delta = 1/\sqrt{2\delta}$  marks the end of renormalization process. The corresponding energy and spatial scales read:

$$\Omega_\delta = \Omega_0 e^{-\frac{\beta}{2\sqrt{2\delta}}}, \quad L_\delta = L_0 e^{\frac{1}{2\sqrt{2\delta}}}. \tag{71}$$

At  $L \gg L_\delta$  interaction between islands is too weak to change the distribution of the relaxation rates, while the ratio of the decimation rates  $q(\tau)/p(\tau)$  starts to drop fast with  $L$ . Density of surviving islands drops with decrease of  $\Omega$ , according to Eqs. (64), (68) as (see Eq. (65)):

$$n_+(\tau_\Omega) = n_0 \left( \frac{\Omega}{\Omega_0} \right)^{2/\beta} \frac{\delta}{\sinh^2 \left( \frac{\sqrt{2\delta}}{\beta} \ln \frac{\Omega_0}{\Omega} \right)}. \tag{72}$$

For the average number of islands inside a cluster,  $N(\tau)$ , we use Eqs. (106) to obtain

$$N_+(\tau_\Omega) = \frac{3}{2\delta} \left[ \tau_\Omega \sqrt{\frac{\delta}{2}} \coth \left( \tau_\Omega \sqrt{\frac{\delta}{2}} \right) - 1 \right] \approx \begin{cases} \frac{1}{4} \tau_\Omega^2 & \tau_\Omega \ll \delta^{-1/2} \\ \frac{3}{2\sqrt{2\delta}} \tau_\Omega & \tau_\Omega \gg \delta^{-1/2} \end{cases} \tag{73}$$



First line above corresponds to the close vicinity of the critical line, and the result  $N_+(\tau) \propto \tau^2$  coincides with the one present in Ref. [22]. The second line demonstrates that logarithmic growth of  $N_+(\tau_\Omega)$  continues even at arbitrary low energy scales, where  $\xi(\tau_\Omega)$  saturates and both  $q(\tau_\Omega)$  and  $n_+(\tau_\Omega)$  vanish.

We do not determine here the dependence of the key RG parameter  $\delta$  on the original parameters like  $\delta_0$  and  $g$ . This dependence may occur to be nontrivial, and we leave this question for future studies.

#### 4.3. Superconducting phase: slow runaway of the RG flow

At negative values of  $\delta$ , the RG equation (62) has qualitatively different solution

$$\xi(\tau) = \sqrt{2|\delta|} \cot \left( \sqrt{\frac{|\delta|}{2}} (\tau + \tau_-) \right), \quad (74)$$

$$q(\tau) = \frac{|\delta|}{\sin^2 \left( \sqrt{\frac{|\delta|}{2}} (\tau + \tau_-) \right)}. \quad (75)$$

Integration constant  $\tau_- \sim 1$  can be ignored at  $|\delta| \ll 1$  for the same reason as described above for  $\tau_+$ . The solution (74) for  $\xi(\tau)$  changes sign at  $\tau = \tau_0 \approx \pi/\sqrt{2|\delta|}$ , while  $q(\tau)$ , has a minimum at the same  $\tau$ . In a broad vicinity of  $\tau_0$ , the function  $q(\tau)$  is nearly constant, which translates to a weak temperature dependence of  $q_T$  in a broad range of low temperatures.

Density of surviving islands behaves now as

$$n_-(\tau_\Omega) = n_0 \left( \frac{\Omega}{\Omega_0} \right)^{2/\beta} \frac{\delta}{\sin^2 \left( \frac{\sqrt{2\delta}}{\beta} \ln \frac{\Omega_0}{\Omega} \right)}. \quad (76)$$

For the average number of islands  $N_-(\tau_\Omega)$  in a typical cluster, we use Eq. (108):

$$N_-(\tau_\Omega) = \frac{3}{2|\delta|} \left[ 1 - \tau_\Omega \sqrt{\frac{|\delta|}{2}} \cot \left( \tau_\Omega \sqrt{\frac{|\delta|}{2}} \right) \right]. \quad (77)$$

At large  $\tau > \tau_0$  superconducting correlations (measured by  $q(\tau)$ ) start to grow, and  $p(\tau) = 1 + \xi(\tau)$  decreases. Near the point  $\tau = 2\tau_0$  the solution (74), (75) develops a singularity. Average number of islands in a typical cluster,  $N_-(\tau)$ , also diverges as  $\tau \rightarrow 2\tau_0$ .

Physically, this solution corresponds to emergence of a globally coherent superconducting state with typical value of the zero-temperature order parameter

$$\Delta_\delta(0) = \Omega_0 e^{-\frac{\beta\pi}{\sqrt{2|\delta|}}} \equiv \Omega_0 \left( \frac{\Omega_\delta}{\Omega_0} \right)^{2\pi}. \quad (78)$$

Note that  $\Delta_\delta$  is parametrically smaller than  $\Omega_\delta$  defined by Eq. (71) at the same value of  $|\delta|$ , due to the presence of extra  $2\pi$  in the exponent in Eq. (78). Such a state is very fragile, with extremely low transition temperature,  $T_c(\delta) \sim \Delta_\delta$ .

Upon approach to the point  $\tau_\Omega = 2\tau_0$ , the RG equations (60), (61) and their consequences (76) and (77) lose their applicability. It happens when the inequality  $\xi(\tau) \ll 1$  is not valid anymore. For very small  $|\delta| \ll 1$  it corresponds to  $\tau$  rather close to  $2\tau_0$ , see Eq. (74).

### 5. Strange metal: qualitative discussion

The range of initial parameters leading to the solution, Eqs. (67), (68), of the strong-disorder RG equation, corresponds to the ground-state of the Griffiths type, which is not globally superconducting. It contains clusters of superconducting islands those phases are locked in together by proximity couplings. Sizes of these clusters vary in a broad range, up to the correlation length  $L_\delta$  given by

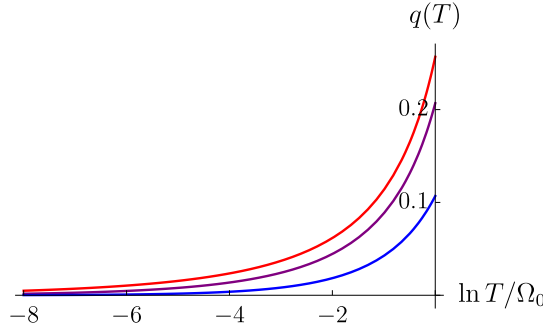


**Fig. 4.** Function  $q(T)$  as found from Eqs. (60), (61) in the normal phase:  $\delta = 0.05, 0.1, 0.2$  from red to blue. (For interpretation of the references to color in this figure legend, the reader is referred to the web version of this article.)

Eq. (71). Typical number of original superconducting islands in the largest clusters is  $N_\delta \sim 1/\delta$ , see Eq. (73) (see Fig. 4).

At any  $T > 0$ , strong-disorder RG flow of Section 4 should be stopped at the lowest energy scale  $\Omega_T = T$ , corresponding to  $\tau_T = (2/\beta)\ln(\Omega_0/T)$ . Interactions of smaller magnitudes,  $J \leq T$ , do not lead to any noticeable phase correlations between clusters which were formed at higher energy scales, i.e. at  $\tau < \tau_T$ . At the final stage of RG, distribution functions (59) which are formed at  $\tau = \tau_T$ , can be rewritten in terms of energy variables  $J$  and  $\gamma$  as follows:

$$\mathcal{P}(\gamma; T)d\gamma = \frac{2p_T}{\beta} \left(\frac{\gamma}{T}\right)^{\frac{2p_T}{\beta}-1} \frac{d\gamma}{T} \tag{79}$$

$$\mathcal{Q}(J; T)dJ = \frac{2q_T}{\beta} \left(\frac{T}{J}\right)^{\frac{2}{\beta}} e^{-q_T\left(\frac{T}{J}\right)^{2/\beta}} \frac{dJ}{J}, \tag{80}$$

where  $(\gamma, J) \leq T$ . Close to the critical point  $p_T \approx 1 + \sqrt{2\delta}$  and  $q_T \ll 1$  is determined by Eq. (68) with  $\tau = \tau_T$ . Eqs. (79), (80) demonstrate that typical value of phase relaxation rate  $\gamma(T) \sim T$ . Typical inter-cluster coupling energy  $J(T) \sim Tq_T^{\beta/2} \ll T$ , demonstrating weakness of interaction between largest clusters.

Observe that Eq. (79) shows that for any  $\beta > 2$ , the exponent  $\frac{2p_T}{\beta}$  always becomes smaller than unity for small enough  $\delta$ , i.e. close enough to the q-SMT critical point (but before the transition point is reached). As soon as  $\frac{2p_T}{\beta} < 1$ , the average correlation time  $\langle 1/\gamma \rangle = \int_0^T \mathcal{P}(\gamma; T)d\gamma/\gamma$  diverges, while  $\langle \gamma \rangle \sim T$ . This divergence does not imply global phase coherence, but rather indicates strong fluctuations of relaxation rates between different clusters. Indeed, correlation time  $t^{(a)}$  of any  $a$ th cluster is bounded from above by its classical value

$$t_a^{cl} = \frac{G_a \hbar}{2\pi T}, \tag{81}$$

which can be found from the action (32) estimating phase diffusion at  $T > 0$ :

$$\frac{1}{2} \langle (\phi_a(0) - \phi_a(t))^2 \rangle \approx \frac{2\pi}{G_a} \frac{T|t|}{\hbar}. \tag{82}$$

Here  $G_a$  stands for the total Andreev conductance (in units of  $4e^2/h$ ) between the  $a$ th cluster of strongly coupled superconducting islands and surrounding normal metal. Since we found previously that Andreev conductances of individual islands  $G_i$  sum up during their ‘merging’ under RG procedure, we expect  $G_a$  to be proportional to the number of islands  $N_a$  constituting  $a$ th cluster. Therefore  $G_a^{max} \sim 1/\delta$ , as follows from Eq. (73) at  $\Omega \sim \Omega_\delta$ . In result, the longest phase correlation

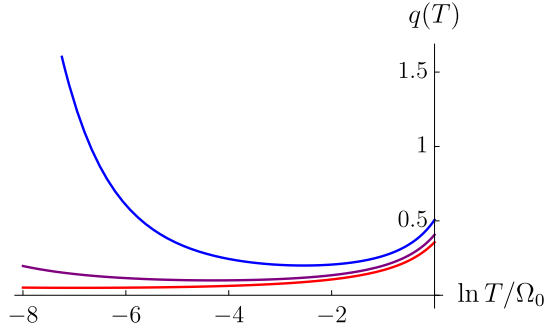


**Fig. 5.** Function  $q(T)$  as found from Eqs. (60), (61) in the superconducting phase:  $-\delta = 0.05, 0.1, 0.2$  from red to blue. (For interpretation of the references to color in this figure legend, the reader is referred to the web version of this article.)

time of largest coupled clusters is estimated as

$$t_{\max}(T) \sim \frac{\hbar}{2\pi T} \frac{1}{\delta}. \tag{83}$$

Note that  $Tt_{\max}(T)$  is singular as  $\delta$  goes to zero, while typical relaxation times  $t_{\text{typ}} \sim \hbar/T$ . This is one of the specific feature of the Griffiths phase characterized by the presence of arbitrary large fractal clusters.

The presence of very large but mutually uncorrelated clusters, leads to an important contribution to the electron dephasing rate  $\tau_\varphi^{-1}$ . Contribution of individual islands to dephasing rate was analyzed in Ref. [48]. Crucial feature of its main result, Eq. (3), is as follows: Andreev reflection contribution to  $\tau_\varphi^{-1}$  is nearly  $T$ -independent at  $T$  much above macroscopic  $T_c$ . The same feature is expected to hold for the Griffiths state with large mutually incoherent clusters.

‘Superconducting’ side of the quantum phase transition is described by Eqs. (74), (75) and demonstrates a very unusual feature: due to the presence of extremum of  $q(\tau)$  at  $\tau_T = \tau_0(\delta) = \pi/\sqrt{2|\delta|}$ , temperature dependencies of physical quantities are expected to be very weak in a broad temperature range

$$T_c = \Omega_0 e^{-\frac{\pi\beta}{\sqrt{2|\delta|}}} \ll T \ll \Omega_0 e^{-\frac{\beta}{2\sqrt{2|\delta|}}}. \tag{84}$$

The relative extension of this range grows enormously as  $|\delta|$  decreases, see Fig. 5. Typical number of islands within largest clusters  $N_a \geq 1/|\delta|$  is the same or larger (see Eq. (77)) than in the Griffiths metal phase, and the above conclusion about nearly- $T$ -independent contribution to the dephasing rate is applicable in the whole interval (84).

We believe that region of phase diagram with small negative  $\delta$ , while being formally superconducting, is a good candidate for the description of a ‘strange metal’ state, for the reasons described in the above paragraph. Note that approximate  $T$ -independence (in the sense described above) comes together with a strong sensitivity to magnetic field: typical scale of magnetic field, which corresponds to a single flux quantum per relevant area,  $L_{\delta_0}^2 = L_0^2 e^{\tau_0}$ , is

$$H_\delta = \frac{\Phi_0}{L_0^2} \exp\left(-\frac{\pi}{\sqrt{2|\delta|}}\right). \tag{85}$$

At  $B \geq H_\delta$  renormalization flow is modified as  $\tau$  reaches  $\tau(B) = \ln(\Phi_0/BL_0^2) < \tau_0(\delta)$ , since proximity coupling becomes frustrated at longer length-scales. In the close vicinity of the critical point  $\delta = 0$  relevant range of magnetic field becomes unexpectedly small. The magnetic field-controlled quantum transition has been studied before [41–43] in the assumption that proximity coupling is short-ranged due to random magnetic frustration. However, at  $T = 0$  exponential decay

of proximity coupling refers to the disorder-averaged  $\langle E_j(r) \rangle$  only, while its second moment is still described [49] by a power-law function of distance  $r$ .

We note that large spatial dimensions of weakly-coupled superconducting clusters makes the system near the critical point unusually susceptible to a weak  $rf$ -frequency noise, like the one demonstrated in Ref. [10].

## 6. Conclusions

We demonstrated breakdown of scaling theory [39] of quantum Superconductor-Metal transition in thin films, due to spontaneous formation of localized islands of superconductivity. The latter is shown to be a generic consequence of sufficiently strong spatial fluctuations of the Cooper attraction strength  $\delta\lambda(\mathbf{r})$  (these fluctuations always become strong [25] close to the mean-field q-SMT via Finkel'stein mechanism [4,5]). This unusual scenario, with a disorder threshold for an appearance of localized Lifschitz tail in the density of locally superconducting regions, is realized when effective Cooper-channel repulsion constant  $\lambda_g = 1/\sqrt{2\pi g} < 1/4$ , corresponding to a normal-state resistivity of a film  $R_{\square} \leq 10$  KOhm. We have also found that the effective strength of fluctuations  $\delta\lambda(\mathbf{r})$  increases with decrease of the electronic mean-free-path  $l$ .

Power-law interaction, see Eq. (50), between phases of different emergent islands, together with power-law distribution of their individual relaxation rates, Eq. (36), lead to formation of a Griffiths-type phase in the vicinity of a genuine transition to superconducting state. This transition is described by a version of Strong-Disorder Renormalization Group, formally similar to the one employed in Refs. [22,45]. Metallic Griffiths phase is described as a line of fixed points of this RG. Physically this phase consists of large fractal clusters of superconducting islands, strongly coupled to each other. The largest size of such clusters is given by  $L_{\delta}$  in Eq. (71), while the number of individual islands in large clusters scales as  $1/\delta$ , where  $\delta$  is the *renormalized* distance to the quantum critical point. Note an important feature of these large fractal clusters: Andreev conductance between such a cluster and surrounding metal is proportional to the number of islands  $N_{\delta}$  it consists of, due to parallel nature of Andreev reflection processes which occur at different islands.

The relation between renormalized parameter  $\delta$  and *bare* distance to the critical point  $\delta_{\text{SCBA}}$  is not yet established; it can be nonlinear. In order to find this relation, one needs to find exact relations between microscopic parameters  $\delta_0$  and  $g$ , and initial conditions  $p(0)$ ,  $q(0)$  for the SDRG equations (60), (61). We leave this interesting problem for future studies.

The most unusual observation of this paper is related to the superconducting phase realized at  $\delta < 0$ . Namely, non-monotonic character of the RG flow in this region of the phase diagram leads to a very weak temperature-dependence of physical properties (including dephasing rate) in a broad range of temperatures, see Eq. (84) and Fig. 5. It might provide a clue to understanding a 'strange metal' phase near q-SMT transition. Below  $T_c$ , a superconducting state occurs. Due to its strong spatial inhomogeneity, we expect it to be gapless, for the reasons understood originally in Ref. [50].

## Declaration of competing interest

The authors declare that they have no known competing financial interests or personal relationships that could have appeared to influence the work reported in this paper.

## Acknowledgments

We are grateful to A. V. Andreev, A. S. Ioselevich, V. E. Kravtsov, M. A. Skvortsov, B. Z. Spivak and S. V. Syzranov for useful discussions. This research was partially supported by the Skoltech NGP grant and by the Russian Academy of Sciences, Russia program 'Modern problems of low-temperature physics'. The research of KT was supported by the Russian Scientific Foundation, Russia, Grant No. 17-72-30036.

## Appendix A. Time-resolved slow dynamics of the two-island system; Appendix B. Strong-disorder renormalization group equations

Supplementary material related to this article can be found online at <https://doi.org/10.1016/j.aop.2020.168138>.

### References

- [1] A.M. Goldman, N. Markovic, *Phys. Today* 51 (1998) 39.
- [2] V.F. Gantmakher, V.T. Dolgoplov, *Phys.-Usp.* 53 (2010) 1.
- [3] I. Burmistrov, I. Gornyi, A. Mirlin, *Phys. Rev. B* 92 (2015) 014506.
- [4] A. Finkel'stein, *JETP Lett.* 45 (1987) 46.
- [5] A. Finkel'stein, *Physica B* 197 (1994) 636.
- [6] M. Feigel'man, A. Larkin, *Chem. Phys.* 235 (1998) 107.
- [7] M. Feigel'man, A. Larkin, M. Skvortsov, *Phys. Rev. Lett.* 86 (2001) 1869.
- [8] B. Spivak, A. Zyuzin, M. Hruska, *Phys. Rev. B* 64 (2001) 132502.
- [9] A. Kapitulnik, S.A. Kivelson, B. Spivak, *Rev. Modern Phys.* 91 (2019) 011002.
- [10] I. Tamir, A. Benyamini, E. Telford, F. Gorniaczyk, A. Doron, T. Levinson, D. Wang, F. Gay, B. Sacépé, J. Hone, et al., *Sci. Adv.* 5 (2019) 1.
- [11] A. Ghosal, M. Randeria, N. Trivedi, *Phys. Rev. B* 65 (2001) 014501.
- [12] M. Feigelman, L. Ioffe, V. Kravtsov, E. Cuevas, *Ann. Physics* 325 (2010) 1390.
- [13] M.V. Feigel'man, L.B. Ioffe, M. Mézard, *Phys. Rev. B* 82 (2010) 184534.
- [14] K. Bouadim, Y.L. Loh, M. Randeria, N. Trivedi, *Nat. Phys.* 7 (2011) 884.
- [15] M. Stosiek, F. Evers, arXiv:1903.10395, 2019.
- [16] M. Feigel'man, M. Skvortsov, K. Tikhonov, *JETP Lett.* 88 (2008) 747.
- [17] D.S. Fisher, *Phys. Rev. Lett.* 69 (1992) 534.
- [18] D.S. Fisher, *Phys. Rev. B* 51 (1995) 6411.
- [19] F. Igloi, C. Monthus, *Phys. Rep.* 412 (2005) 277.
- [20] F. Igloi, C. Monthus, *Eur. Phys. J. B* 91 (2014) 290.
- [21] G. Refael, E. Altman, C. R. Phys. 14 (2013) 725.
- [22] R. Juhasz, I.A. Kovacs, F. Igloi, *Europhys. Lett.* 107 (2014) 47008.
- [23] M. Feigel'man, A. Larkin, M. Skvortsov, *Phys. Rev. B* 61 (2000) 12361.
- [24] Y. Oreg, A.M. Finkel'stein, *Phys. Rev. Lett.* 83 (1999) 191.
- [25] M. Skvortsov, M. Feigel'man, *Phys. Rev. Lett.* 95 (2005) 057002.
- [26] L. Levitov, *Europhys. Lett.* 9 (1989) 83.
- [27] A. Burin, L. Maksimov, *JETP Lett.* 50 (1989) 338.
- [28] L. Levitov, *Phys. Rev. Lett.* 64 (1990) 547.
- [29] S.V. Syzranov, L. Radzihovsky, *Annu. Rev. Condens. Matter Phys.* 9 (2018) 35.
- [30] A. Rodríguez, V. Malyshev, F. Domínguez-Adame, *J. Phys. A: Math. Gen.* 33 (2000) L161.
- [31] A. Rodríguez, V. Malyshev, G. Sierra, M. Martín-Delgado, J. Rodríguez-Laguna, F. Domínguez-Adame, *Phys. Rev. Lett.* 90 (2003) 027404.
- [32] A. Malyshev, V. Malyshev, F. Domínguez-Adame, *Phys. Rev. B* 70 (2004) 172202.
- [33] F. De Moura, A. Malyshev, M. Lyra, V. Malyshev, F. Domínguez-Adame, *Phys. Rev. B* 71 (2005) 174203.
- [34] X. Deng, V. Kravtsov, G. Shlyapnikov, L. Santos, *Phys. Rev. Lett.* 120 (2018) 110602.
- [35] P.A. Nosov, I.M. Khaymovich, V. Kravtsov, *Phys. Rev. B* 99 (2019) 104203.
- [36] X. Deng, A.L. Burin, I.M. Khaymovich, arXiv:2002.00013, 2020.
- [37] I. Suslov, *Zh. Eksp. Teor. Fiz.* 106 (1994) 560.
- [38] S. Syzranov, V. Gurarie, L. Radzihovsky, *Phys. Rev. B* 91 (2015) 035133.
- [39] T. Kirkpatrick, D. Belitz, *Phys. Rev. Lett.* 79 (1997) 3042.
- [40] V.M. Galitski, S. Das Sarma, *Phys. Rev. B* 67 (2008) 144501.
- [41] J.A. Hoyos, C. Kotabage, T. Vojta, *Phys. Rev. Lett.* 99 (2007) 23601.
- [42] J.A. Hoyos, C. Kotabage, T. Vojta, *Phys. Rev. B* 79 (2009) 024401.
- [43] A. Del Maestro, B. Rosenow, M. Müller, S. Sachdev, *Phys. Rev. Lett.* 101 (2008) 035701.
- [44] A.D. Maestro, B. Bernd Rosenow, J.A. Hoyos, T. Vojta, *Phys. Rev. Lett.* 105 (2010) 145702.
- [45] E. Altman, Y. Kafri, A. Polkovnikov, G. Refael, *Phys. Rev. Lett.* 93 (2004) 150402.
- [46] J.M. Kosterlitz, *J. Phys. C: Solid State Phys.* 7 (1974) 1046.
- [47] F. Igloi, *Phys. Rev. B* 65 (2002) 064416.
- [48] M.A. Skvortsov, A.I. Larkin, M.V. Feigel'man, *Phys. Rev. Lett.* 92 (2004) 247002.
- [49] B. Spivak, F. Zhou, *Phys. Rev. Lett.* 74 (1995) 2800.
- [50] A.I. Larkin, Y.N. Ovchinnikov, *Sov. Phys.—JETP* 34 (1972) 1144.